Europace Advance Access published February 9, 2011

Europace
doi:10.1093/europace/eur004

CLINICAL RESEARCH

Three-dimensional coronary sinus reconstruction-guided left ventricular lead implantation based on intraprocedural rotational angiography: a novel imaging modality in cardiac resynchronization device implantation†

Klaus-Jürgen Gutleben[1,2]*, Georg Nölker[1], Guido Ritscher[1], Harald Rittger[1], Christopher Rohkohl[3], Günter Lauritsch[4], Johannes Brachmann[1], and Anil Martin Sinha[1]

[1]Klinikum Coburg GmbH, Coburg, Germany; [2]Clinic for Cardiology, Heart and Diabetes Center North Rhine-Westphalia, Ruhr University of Bochum, Georgstr. 11, 32545 Bad Oeynhausen, Germany; [3]Pattern Recognition Lab, Friedrich-Alexander-University, Erlangen, Germany; and [4]Siemens AG, Health Sector, Forchheim, Germany

Received 31 August 2010; accepted after revision 31 December 2010

Aims Rotational angiography (RA) of the coronary sinus (CS) provides more anatomical insights compared with static angiographies. We evaluated intraprocedural three-dimensional (3D) CS reconstruction (RC) based on RA, using syngo® DynaCT Cardiac to guide CS lead implantation.

Methods and results In 24 patients with indication for cardiac resynchronization therapy, intraprocedural RA and 3D RC of the CS was performed. Lead placement was guided by 3D image integration into real-time fluoroscopy. Rotational angiography and 3D RCs were evaluated regarding visibility of the CS and tributaries, CS-to-target vein angles, and vessel diameters. The target vein for CS lead implantation, identified by RA, was successfully displayed by 3D RC in 20 (91%) of 22 patients with adequate RA. All lead implantations were guided successfully by 3D image integration into real-time fluoroscopy. Cranial or caudal angulations were used in 95% of the procedures without further angiographies. Rotational angiography displayed a mean of 2.9 $\pm$ 1.0 second-order side branches compared with 1.8 $\pm$ 1.1 in 3D RCs ($P < 0.05$). The CS-to-target vein angle estimated from static projections (right anterior oblique 20°, left anterior oblique 40°, and even optimal RA view) differed substantially from 3D RCs. Main vessel diameters did not differ significantly between both techniques.

Conclusion Intraprocedural 3D RC of the CS and 3D image integration-guided lead placement is feasible. Coronary sinus-to-target vein angles seemed to be misestimated even by RA views compared with 3D RC. Thus RA and 3D CS RC should be applied routinely for CS lead implantation.

Keywords Congestive heart failure • Cardiac resynchronization therapy • Rotational angiography • Coronary sinus three-dimensional reconstruction • image integration

Introduction

Cardiac resynchronization therapy (CRT) is recommended as a helpful treatment option in patients with severe heart failure and conduction disturbances,[1] but also in patients with mild heart failure symptoms.[2–4] Transvenous implantation of coronary sinus

†Data were presented at the 17th World Congress in Cardiac Electrophysiology & Cardiac Techniques, Nice, France.

* Corresponding author. Tel: +49 5731 97 0; fax: +49 5731 97 2300, Email: gutleben@gmx.de

(CS) pacing electrodes has become the most frequently used approach to establish left ventricular (LV) or biventricular pacing. However, despite modern implantation tools LV lead-related complications remain substantial in numerous patients[2] and therapy failure rates are known to be about 30%.[5] The success rates of CRT have been shown to be influenced by the contraction pattern and scar burden of the LV as well as the relationship between LV pacing lead position and the area of latest LV activation.[6–8] Moreover, the pacing site within the posterolateral wall region of the LV also seemed to influence the benefit of CRT.[8,9] Thus, an optimal LV pacing position is crucial regarding success rates of biventricular pacing.[8–10] For establishing the best pacing lead position especially in acutely angulated and tortuous veins, precise information about the cardiac venous tree anatomy is required. The most frequently used modality to visualize the coronary venous tree anatomy for transvenous lead placement was conventional venography with or without balloon occlusion. But also multirow computed tomography,[11,12] cardiac magnetic resonance tomography imaging,[13,14] and rotational angiography (RA)[15–17] have been successfully used. An enormous variability of the CS and its tributaries has been demonstrated.[13,16] Rotational angiography has been shown to provide more anatomical information as compared with static standard angiography views,[16] and proved to be helpful in CS lead implantation.[17] DynaCT Cardiac® (Siemens, Forchheim, Germany) has been introduced as a new technique for RA and three-dimensional (3D) reconstruction (RC) of cardiac structures, providing reliable anatomic information for interventional procedures.[18] However, there are no data available about the use of DynaCT Cardiac for CS evaluation in CRT patients.

The aims of this study were to evaluate the feasibility of 3D RC of the CS obtained from intraprocedural RA using syngo® DynaCT Cardiac (Siemens, Forchheim, Germany). Procedural success of 3D RCs, image integration into real-time fluoroscopy, and image integration-guided transvenous lead implantation were analysed. Moreover, we compared static angiography, multiangle RA, and 3D RC views, regarding visibility of the main CS branches, vessel diameters, and CS-to-target vein angles.

Methods

Study population

After obtaining ethical approval by the regional ethical committee and informed consent, patients with indication for CRT according to the current guidelines[1] were included in the study. They received intraprocedural RA, 3D RC of the coronary venous tree, and 3D CS RC image integration into real-time fluoroscopy to guide transvenous lead implantation.

Rotational angiography and three-dimensional reconstruction

After balloon occlusion of the CS between the tributary of the LV posterior vein and the left marginal vein, contrast media (Ultravist 370, Bayer-Schering GmbH, Berlin, Germany) was applied manually through the balloon catheter. Once the contrast media opacified also the peripheral parts of the venous tree, RA using syngo® DynaCT Cardiac (Siemens) was started. Isocentric rotation of the detector acquired 398 frames over an angle of 198° [99° right anterior oblique (RAO) to 99° left anterior oblique (LAO)] in a single 8 s run under breath hold condition (*Figure 2*). Three-dimensional RC of the CS was performed immediately after RA, using syngo® InSpace software (Siemens, Forchheim, Germany) and a newly developed motion-compensated ECG gated algorithm.[19] Three-dimensional RC provided additional views, including any caudal and cranial angulations without further contrast media applications.

Measurements

Visibilities of the CS, posterior interventricular veins, LV posterior veins, and left marginal veins were compared between multiangle RA and 3D RC views. Additionally, the number of second-order branches tributaring into posterior interventricular veins, LV posterior veins, and left marginal veins were compared between both imaging modalities.

Coronary sinus-to-target vein angles were measured in two static angiograpic views from an RA run (RAO 20°, LAO 40°) and an optimal RA view. The latter was identified by screening the entire RA run for the angulation that was (i) adjustable and (ii) displaying the CS-to-target vein angle mirroring the true angle. The phase of the cardiac cycle depended on the phase of the RA since the whole run of 198° was displayed by 298 frames. For angle assessments, the tributaring sites of the vessels and CS met in the vertex of the angles. The arms of an angle were defined by the vertex and a point that was either 1 cm distally in the target vein or 1 cm proximally in the CS. Measurements were compared with the angles obtained from 3D RC. These values were measured after adjusting the angulation three dimensionally to an orthogonal view allowing for measurements of true angles.

Coronary sinus diameters at the ostium and at tributaring sites of all posterior LV and left marginal target veins were measured as well as the diameters of the branches at the site of tributaring into the CS. Measurements were calibrated on the known diameter of the guiding catheter. Left anterior oblique 40° was used to measure diameters of the CS. Best RA views served as angulations for side-branch measurements. The same angulations were used in 3D RC measurements.

The measurements were performed in the same way in patients independent of sinus rhythm or atrial fibrillation. The measurements in 3D RC were performed by a second experienced observer, who was blinded for the values obtained from RA. *Figure 1* summarizes the workflow of the study procedures.

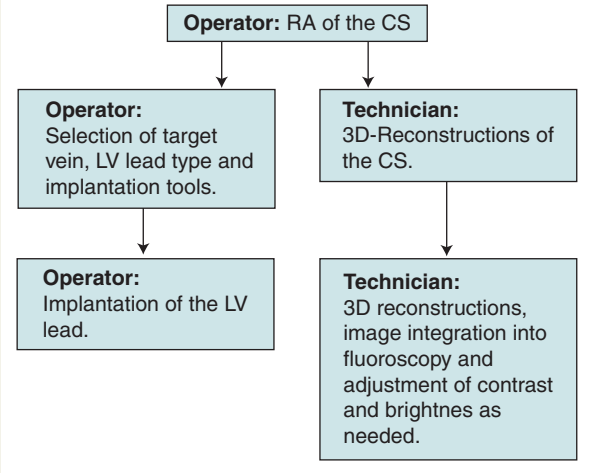

Figure 1 Flow chart of the study-specific procedure.

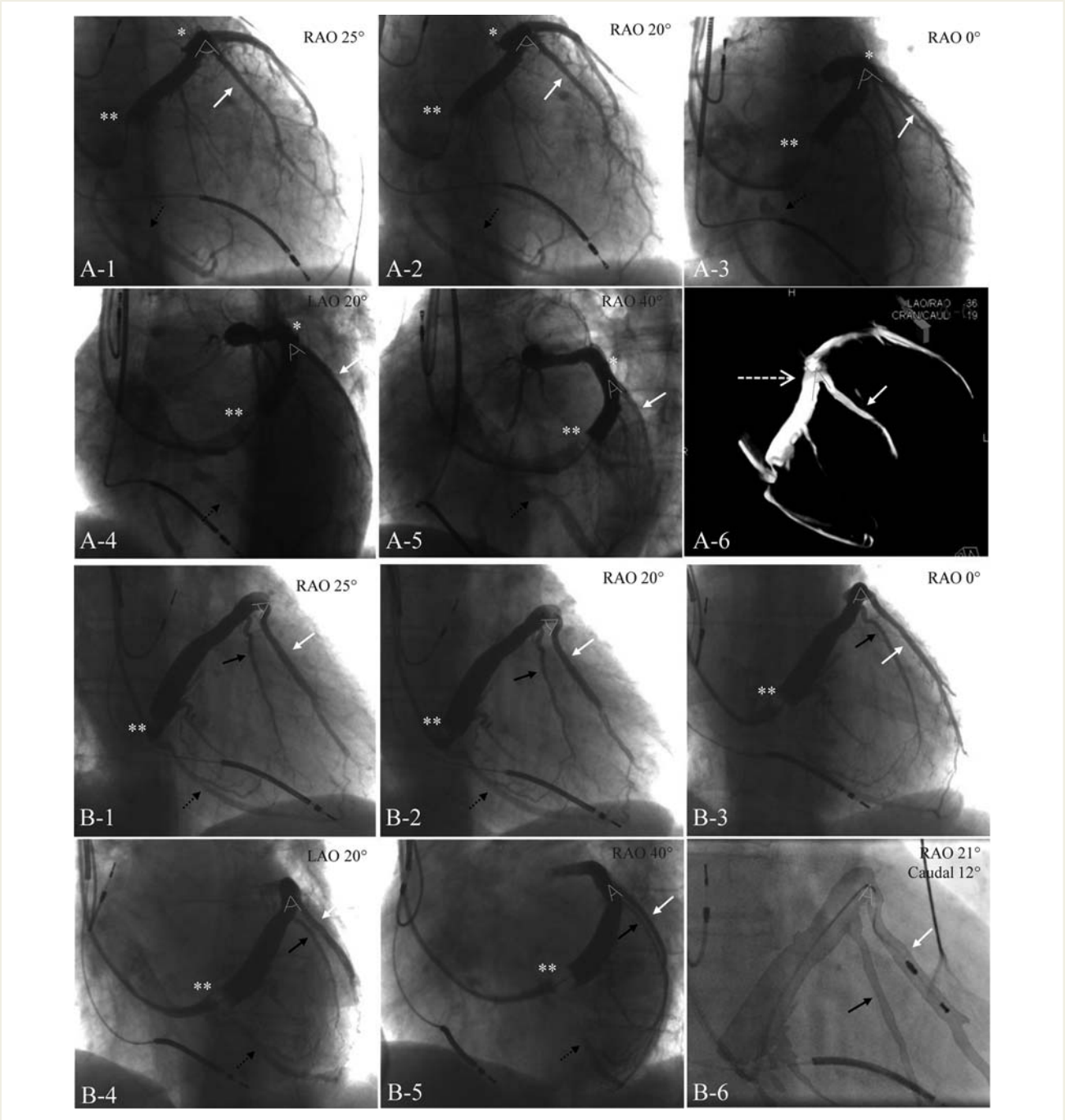

Figure 2 Angiography views from RA, 3D RCs, and 3D image integration into fluoroscopy to guide LV lead placement in Patients 16 (A1–A6) and 23 (B1–B6). Different RA views from Patient 16 show a vessel overlap (*) in the tributaring region of the prominent left marginal target vein into the CS with a tortuous part of the anterior vein (A1–A5). This hampered the assessment of this challenging anatomic region, whereas 3D RC (A6) depicted this area in high spatial resolution in an RAO 36° and caudal 19° angulation without vessel overlap (dotted arrow). RA views from Patient 23 (B1–B5) depict a prominent left marginal target vein with an acute CS-to-target vein angle. Image integration into real-time fluoroscopy facilitated LV pacing lead placement using the optimal projection of RAO 21° and caudal 12° (B6). RA, rotational angiography; 3D, three dimensional; LV, left ventricular; RAO, right anterior oblique; *, vessel overlap of the target vessel with a tortuous part of the anterior vein; **, inflated occlusion balloon within the CS; white arrow, left marginal target vein; white dotted arrow, tributaring region of LMV; black arrow, alternative left marginal target vein; dotted black arrow, alternative posterior target vein of the left ventricle.

Arterial vs. venous contrast media application for rotational angiography and three-dimensional reconstruction

In one patient, RA and 3D RC of the CS additionally were performed during the venous phase of left coronary artery angiography 2 days prior to the implantation procedure. Intraindividual comparisons between both RAs and 3D RCs were made in this case. Visibility of the CS and its branches as well as CS and branch diameters were compared between both antegrade and retrograde multiangle RA views and 3D RCs obtained from the two different RA modalities.

Data analysis

The number of CS tributaries as well as vessel diameters were compared between multiangle rotational angiographic views and 3D RCs using Student's *t*-test for independent samples. For CS-to-target vessel angles, Pearson's correlation was performed. A *P*-value <0.05 was considered statistically significant. Statistical analysis was performed using the SPSS 16.0 software (SPSS Inc., Chicago, IL, USA).

Results

Patient characteristics

A total of 24 patients were enrolled in the study between June 2008 und February 2009. Patient characteristics are listed in *Table 1*. All patients fulfilled criteria for CRT according to common guidelines.[1]

Procedure

All procedures were under local anaesthesia conditions, with intravenous analgesia and sedation added as needed, and performed by the same physician. After accessing the right or left subclavian vein, standard leads were placed into the right atrium and the right ventricular apex at first. Then LV leads (Attain® 4194 and 4196, Medtronic, Inc., Minneapolis, MN, USA; Corox® OTW-S, Biotronik, Berlin, Germany; Quickflex®, St Jude Medical, St Paul, MN, USA; Situs™ OTW, Sorin, Paris, France) were implanted using standard guiding catheters (Attain® 6227 DEF, Medtronic, Inc., Minneapolis, MN, USA; ScoutPro®, Biotronik, Berlin, Germany; CPS Aim™, St Jude Medical, Inc., St Paul, MN, USA; Situs LDS 2, Sorin, Paris, France) after RA and 3D RC of the CS.

Table 1 Patient characteristics

Characteristics	Value
No. of patients	24
Age (mean ± standard deviation)	68 ± 11 years
Gender (male/female)	22/2
Atrial fibrillation	5/24 (21%)
Coronary artery disease	12/24 (50%)
Ejection fraction (mean ± standard deviation)	24 ± 8%
QRS duration (mean ± standard deviation)	159 ± 27 ms
NYHA class symptoms	3 ± 1

NYHA, New York Heart Association.

Coronary sinus pacing lead implantation

The best target branch was defined as giving access to the lateral or posterolateral region with adequate size and morphology for lead implantation. It was identified from multiangle RA views. Difficulties in anatomy assessment using RA views due to vessel overlap were supplemented by 3D RC views (*Figure 2A*). Posterior veins of the LV and left marginal veins were selected in 9 and 15 cases, respectively. Rotational angiography views, 3D RCs, and image integration of 3D RCs into real-time fluoroscopy were used as reference for pacing lead implantation. Syngo® ipilot software (Siemens, Forchheim, Germany) was used for image integration (*Figure 2B*) and offered additionally any caudal and cranial angulation as a reference view that was possible to adjust. Optimal angulations were individually adjusted and adapted as needed according to the anatomy of the target branch leading to the favourable pacing site. Angulations for accessing the target vein included cranial angulations of 11 ± 7° in 7 cases and caudal angulations of 16 ± 6° in 12 cases. In left marginal target veins, RAO (5 ± 20°) and caudal (13 ± 9°) angulations were used. The LAO and cranial projections were used less frequently compared with RAO and cranial projections, respectively (four vs. nine patients). In contrast, all posterior veins of the left ventricle required LAO (21 ± 7°) and cranial (12 ± 6°) angulated projections when used as target veins (*Figure 3*). Using this approach, all leads were successfully implanted into the initially targeted veins with a lead tip position in the lateral or posterolateral region. There was no unacceptable phrenic nerve stimulation after final lead positioning.

Rotational angiography of the venous phase during coronary artery angiography

In one patient, additionally RA from the venous phase after contrast media injection into the left coronary artery during coronary angiography was performed. Rotational angiography was manually started 5 s after contrast media injection. This delay was found to be the time difference between contrast media injection and CS opacification in conventional left coronary artery angiography. Coronary sinus was reconstructed and 3D image was integrated into real-time fluoroscopy during CRT device implantation 2 days later. Thus, CS intubation additionally was guided by image integration.

Prevalence of the coronary sinus and its tributaries

Visibility of the CS and its branches are summarized in *Table 2*. Since 3D RC of the coronary venous tree was based on RA, fewer branches were depicted by 3D RC. However, target veins, selected by RA, were successfully reconstructed in the majority of cases (20 of 22 patients, 91%). Using RA, 2.9 ± 1.0 second-order side branches with a diameter ≥1 mm were detected per patient compared with 1.8 ± 1.1 in 3D RC views ($P < 0.05$).

Second-order side branches tributaring into left marginal veins were most likely depicted in 3D RCs (80%) compared with second-order side branches tributaring into posterior veins of the

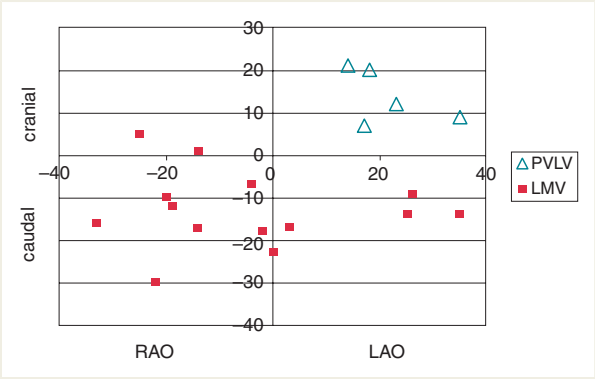

Figure 3 Distribution of optimal angulations to guide pacing lead implantation. Left marginal veins (squares) needed more right anterior oblique (left side) and caudal (upper part of the panel) angulations, whereas all pacing lead implantations into posterior veins of the left ventricle (triangles) were guided by left anterior oblique (right side) and cranial angulations (lower part).

Table 2 Comparison of rotational angiography and three-dimensional RCs regarding visibility of the main branches and vessel diameter

Visibility	RA	3D (*n*, %RA)
CS	24	22 (92%)
PIV	23	13 (57%)
PVLV	18	9 (50%)
LMV	21	14 (67%)
Target vein	22	20 (91%)
Second-order branches tributaring into PIV	12	4 (33%)
Second-order branches tributaring into PVLV	15	9 (60%)
Second-order branches tributaring into LMV	40	32 (80%)
Total number of second-order branches	67	45 (67%)
Diameter (mm, mean ± SD)	RA	3D RC
CS-Os	14.7 ± 3.7	16.0 ± 3.9
CS at PVLV	10.3 ± 3.2	9.5 ± 1.5
CS at LMV	8.8 ± 1.9	8.3 ± 1.7
PVLV	4.5 ± 1.0	4.3 ± 0.5
MLV	4.7 ± 0.8	4.8 ± 0.9

RA, rotational angiography; 3D, three dimensional; CS, coronary sinus; PIV, posterior interventricular vein; PVLV, posterior vein of the left ventricle; LMV, left marginal vein; CS-Os, coronary sinus ostium.

left ventricle (60%) and posterior interventricular veins (33%). The reasons for partial poor image quality were small collateral branches between lateral, anterolateral, and posterolateral tributaries in five cases, instable balloon position in two patients, and venous valves in two patients, and a start of RA before contrast media was distributed within the small CS branches. Conventional selective venographies were used to identify target vessels in two of these patients.

Vessel diameters

Vessel diameters of the CS ostium, the CS at tributaring posterior LV and left marginal target veins as well as diameters of all target veins at the tributaring site are listed in *Table 2*. There were no statistically significant differences between both imaging modalities.

Coronary sinus-to-target vein angles

Angles between CS and selected target veins are depicted in *Figure 4*. Angles were measured in static projections from RA (RAO 20°, LAO 40°, and optimal RA view). The values were compared with measurements from 3D RCs. Angle differences between RAO 20°, LAO 40°, and best RA compared with 3D RC were 8 ± 28°, 8 ± 27°, and 14 ± 32°, respectively. Angle differences of more than 15° were detected in 9, 11, and 7 patients by RAO 20°, LAO 40°, and best RA view. Acute angles, defined as angles <90°, were detected in 7, 8, and 5 patients by RAO 20°, LAO 40° RA compared with 5 in 3D RCs. Regarding this parameter, RAO 20°, LAO 40°, and even best RA views lead to misestimations in one, six, and three patients.

Influence of vessel overlap and tortuosity

Figure 2 displays RA projections from Patient 16. This film showed vessel overlap with a part of the anterior coronary vein over the whole run (*Figures 2A1–5* and *4*). This led to a moderate misestimation of the angle (*Figure 4*). Patient 6 showed a tortuosity at the tributaring region of the target vein, which was only unmasked by 3D RC. Due to this vessel overlap, large differences of up to 79° were obtained in the comparison of static projections from RA and 3D RCs. This leads to a substantial misestimation in this patient (*Figure 4*).

Arterial vs. venous contrast media application for rotational angiography and three-dimensional reconstruction

Three-dimensional RC of the CS from RA after contrast media application into the left coronary artery allowed for successful 3D image integration into fluoroscopy to guide CS cannulation. Parameters comparing these two imaging modalities are listed in *Table 3*. Image quality was sufficient for visualization and 3D RC of the most important of the second-order branches in both modalities. However, 3D CS RC after balloon occlusion RA allowed a more homogeneous depiction of the coronary venous tree, with a higher spatial resolution of the first- and second-order branches being visualized over a longer distance compared with 3D RC after arterial contrast media injection. Moreover, 3D RC from RA after arterial contrast media application was more difficult compared with venous balloon occlusion RA of the CS. These differences were due to the opacification of the contrast media within the venous system and the amount of contrast media remaining within the coronary arteries during the venous phase.

Procedural data on fluoroscopy time dosage and procedure time

The total procedure and fluoroscopy times were 192 ± 69 and 41 ± 25 min, respectively. The times needed for RA and LV lead placement were 11 ± 7 and 35 ± 32 min, respectively. The total

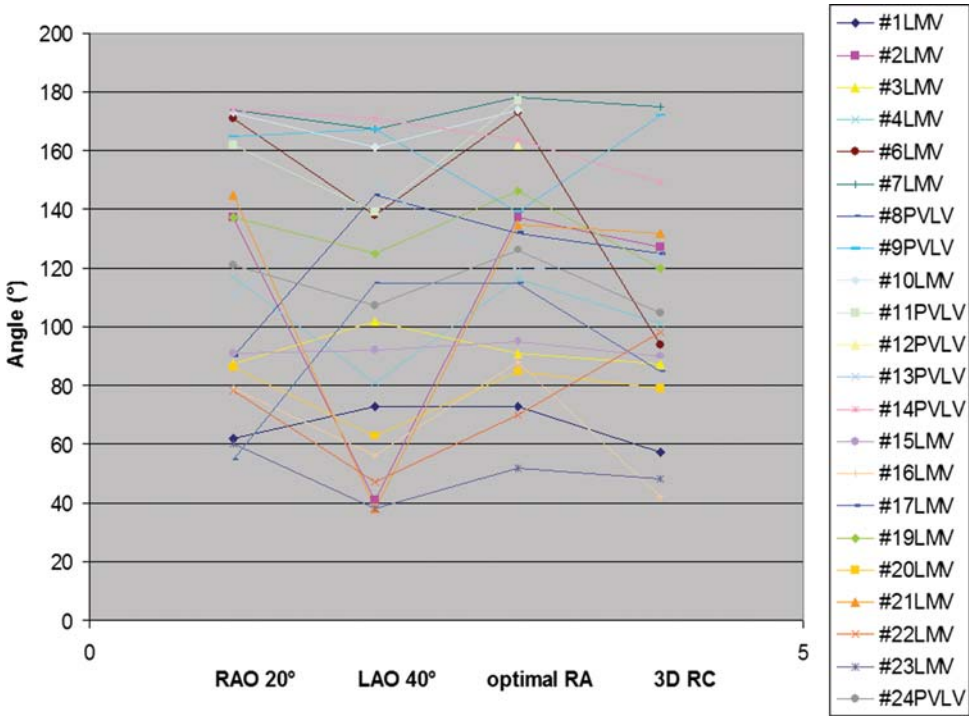

Figure 4 Coronary sinus-to-target vein angle measurements from right anterior oblique 20°, left anterior oblique 40°, optimal rotational angiography, and three-dimensional RC views. Note that intraindividual estimations of target vein angles vary to a large extent in different modalities.

radiation exposure was 10426 ± 5628 cGy m^2. The mean amount of contrast agent needed for RA was 11 ± 1 mL. There were no significant differences between patients with left marginal or posterior veins of the left ventricle used as target veins.

Procedural complications

During the procedures, no acute complications occurred. However, one LV lead dislodgement needed replacement before hospital discharge. An alternative target vein was used successfully in this case.

Discussion

The main findings of our study were that 3D CS RC-guided LV pacing lead placement based on intraprocedural RA was feasible and helpful in the majority of our patients. Three-dimensional RCs depicted the majority of target vessels. The availability of any caudal and cranial reference view without further venographies and image integration into real-time fluoroscopy improved successful guiding of the transvenous CS lead placement, whereas conventional venographies, including multiangle RA view, led to misestimations of the CS-to-target vein angle compared with 3D RCs.

Blendea *et al.*[16] studied the variability of the coronary venous tree using RA in patients undergoing CRT. They pointed out that anatomic differences between certain patient groups could be of importance for LV lead placement. The main CS branches (CS, posterior interventricular veins, posterior veins of the left ventricle, and left marginal veins) were depicted with a similar prevalence compared with our RA results. However, 3D RCs from RA were not described.[16]

More recently Lumia *et al.* reported multidetector computed tomography investigations, primarily performed to diagnose coronary artery disease. Retrospectively the visualization of CS branches was analysed in a cohort of 89 patients. Left lateral and posterior interventricular veins were depicted in 67 and 75%, respectively, which was less often compared with our results.[12] Due to the retrospective analysis, there was no comparison with invasive venographies.

Although 3D RCs in our study displayed fewer CS branches compared with RA, the majority of target veins (91%) were also detected by this modality. Rotational angiography displayed 2.9 ± 1 second-order side-branch tributaring into posterior interventricular veins, posterior veins of the left ventricle, and left marginal veins per patient compared with 1.8 ± 1.1 (67 %) in 3D RCs. Van de Veire *et al.* performed multislice computed tomographies to visualize the coronary venous tree in 21 patients scheduled for CRT and compared the results with invasive venographies. Vessel analysis detected 1.6 second-order side branches of posterior interventricular veins, posterior veins of the left ventricle, and left marginal veins per patient compared with 2.0 in invasive venographies. These values were somewhat lower compared with the values from RAs and 3D RCs in our study. Coronary sinus-to-target vein angles, the impact of caudal and cranial angulations, as well as 3D image integration to guide LV lead placement were not evaluated by Van de Veire *et al.*[8]

Table 3 Comparison rotational angiographys and three-dimensional RCs after antegrade contrast media application during left coronary artery angiography and conventional retrograde contrast media application with balloon occlusion of the coronary sinus. Number of investigated patients: $n = 1$

	RA_{ante}	RA_{retro}	$3D_{ante}$	$3D_{retro}$
Visibility (no. of branches)				
CS	1	1	1	1
PIV	0	1	0	0
PVLV	1	1	1	1
LMV	2	2	2	2
Second-order branches	2	6	2	4
Diameter (mm)				
CS-Os	9.4	–	9.5	–
CS-PVLV	–	13.2	–	12
CS-LMV1	6.0	9.3	5.7	7.6
PVLV	–	5.8	–	3.7
LMV1	5.3	5.3	5.2	4.7

RA, rotational angiography; 3D, three dimensional; CS, coronary sinus; RA_{ante}, RA after antegrade contrast media application through left coronary artery; RA_{retro}, RA with retrograde contrast media application with balloon occlusion of the CS; PIV, posterior interventricular vein; PVLV, posterior vein of the left ventricle; LMV, left marginal vein; CS-Os, CS ostium; CS-PVLV, CS at posterior vein of the left ventricle; CS-LMV1, CS at first left marginal vein; CS-PVLV, CS at tributaring posterior vein of the left ventricle; CS-LMV1, coronary sinus at tributaring first left marginal vein; –, no value.

Contrast media application in RA with balloon occlusion within the proximal CS bears the risk of imbalanced contrast media opacification. This might be due to the fact that contrast media flow in left marginal veins is usually directed against the normal blood flow. Posterior veins of the left ventricle and posterior interventricular veins however are opacified with the normal blood flow after contrast media has passed lateral or anterolateral veins.

This might influence the prevalence and diameters of certain branches and limit the comparison of balloon occlusion venography with computed tomography, magnet resonance studies, and RA of the venous phase during coronary artery angiography.

The tributaring region of the target vessel with acute angulation, vessel overlap in conventional venography, and tortuosity are known to be challenging in transvenous pacing lead implantation.[10] Studies of Blendea *et al.* have shown that CS-to-target vein angles were misclassified in 5 posterior and 11 lateral target veins in 49 patients by conventional venography compared with RA. The authors concluded that RA, offering multiple views from the coronary venous tree from multiple angles, could better identify the angulations of the various branches.[17] In our studies, RAO 20°, LAO 40°, and best RA views detected acute CS-to-target vein angles in seven, eight, and five patients, respectively, compared with five in 3D RCs. Within the latter five patients, RAO 20°, LAO 40°, and multiangle RA views did not match the parameter of an acute angle in one, six, and three patients. Additionally, a CS-to-target vein angle deviation of more than 15° between multiangle RA views and 3D RCs was found in five patients. These findings indicate that conventional venographies and even multiangle RA views lead to misinterpretation of the desired anatomic region. In two of our patients, the problems of vessel overlap and/or vessel tortuosity at vessel tributaries were evident, which might lead to a misestimation of the angle. Three-dimensional RC has the potential to display the true anatomy.

These results support the hypothesis that vessel angles can only be accurately determined after 3D assessment of the planes the angles are covered with.

In our study, contrast agent consumption for RA was lower (11 ± 1 mL) as reported from earlier investigations with other RA techniques (20–40 mL of diluted contrast dye).[15,16,20] In multislice computed tomography, an even larger amount of contrast dye consumption (108 ± 11 mL) was needed.[8]

Radiation exposure during RA was higher compared with two standard projections, but was comparable with that of standard angiographies of the same duration.[16] In an earlier patient cohort, we studied selective cannulation of the target vessel for LV lead implantation.[21] Within that historic control group, the total fluoroscopy (30 ± 17 vs. 41 ± 25 min) and procedure times (159 ± 43 vs. 192 ± 69 min) were shorter, whereas the LV lead implantation time was longer compared with this study using RA and 3D RC (56 ± 34 vs. 35 ± 32 min). Shorter LV lead implantation times using RA and 3D RCs also suggested that the experience of the operator and improvement of implantation tools might have influenced procedural outcome.

Duray *et al.*[22] reported that implantation success in the first choice CS side branch was 71% in a series of 77 patients. The higher success rate targeting the first choice side branch in our smaller group of patients may be due to the fact that the target side branch for LV lead implantation was identified from multiangle RA view giving more information on the anatomy of the vessel compared with static venographies.

Clinical implication

Using this technique, we could confirm the value of RA of the CS for LV pacing lead implantation as reported by others.[17] To guide LV lead placement, cranial or caudal angulations were used in the majority of patients. These additional angulations were available without further angiographies or need for additional contrast media after 3D RCs from RA. Moreover, image integration of 3D RCs into real-time fluoroscopy optimized spatial orientation and navigation of guide wires and pacing leads through the CS. Three-dimensional RCs provided additional anatomical information and helped in assessing complex anatomic regions of the coronary venous trees. According to the CS-to-target vein analysis in a conventional setting without RA, LAO and cranial projections should be considered if additional venographies are needed to guide LV lead placement in a posterior vein of the left ventricle. For left marginal veins, additional venographies should rather include RAO and caudal angulations. However, venographies should be performed in two standard projections, including LAO (e.g. 40°) and RAO (e.g. 20°), since the target vein was unclear at that point of time.

Additionally, RA from the venous phase of left coronary artery angiography provided the opportunity of image integration-guided CS cannulation, which might reduce implantation procedure duration.

Optimal angulations for accessing the target vein included LAO and cranial angulations in all the posterior target veins of the left ventricle, whereas left marginal target veins needed more RAO and caudal projections. This finding should be confirmed in further studies and might have an influence on the procedural approach in the future.

Limitations

In our study, static projections were part of the RA run and thus consisted of only one frame. This might limit the comparison of static angiography views with other modalities. Two separate angiographies would have been associated with a higher amount of contrast media consumption and radiation exposure.

Although the times needed for RA and 3D RC were relatively low, additional time for this approach might be a limitation.

Three-dimensional RC was able to display the majority of selected target veins with high spatial resolution. This allowed for a precise assessment of vein anatomy, especially regarding the tributaring region including angle measurements. For alternative target veins, RA seemed to improve the implantation procedure, although 3D RC seemed unreliable in some of the cases.

For intraprocedural 3D RC and image integration, an additional person was available in our study. This might limit this approach in clinical routine.

Due to the design of our study and the limited number of patients, we were not able to assess the influence of 3D RC on the total procedure time or success rates. To examine this question, further investigations with different study groups and larger cohorts of patients will need to be performed.

Conclusion

We described for the first time intraprocedural CS RC from RA for CS lead implantation in CRT patients. This novel technique provided high spatial resolution of the CS and its tributaries with a limited amount of contrast media consumption.

Additional anatomic information was provided, including caudal and cranial angulations without further venographies. This might facilitate CS lead advancement, especially in acute angulated and tortuous target veins. Three-dimensional RC of the cardiac venous tree from RA after contrast media application into the left coronary artery was also feasible and provided the possibility of CS intubation guided by image integration of 3D RC of the CS into realtime fluoroscopy.

Conflict of interest: G.N. and A.M.S. obtained fees for lectures from Siemens AG. K.C. had a collaboration contract with Siemens AG and G.L. was an employee of Siemens AG. C.R. was a freelancer of Siemens AG.

References

1. Hunt SA, Abraham WT, Chin MH, Feldman AM, Francis GS, Ganiats TG *et al.* 2009 Focused update incorporated into the ACC/AHA 2005 guidelines for the diagnosis and management of heart failure in adults: a report of the American College of Cardiology Foundation/American Heart Association Task Force on practice guidelines: developed in collaboration with the international Society for Heart and Lung Transplantation. *Circulation* 2009;**119**:e391–479.
2. Linde C, Abraham WT, Gold MR, St John Sutton M, Ghio S, Daubert C. REVERSE (REsynchronization reVErses Remodeling in Systolic left vEntricular dysfunction) Study Group. Randomized trial of cardiac resynchronization in mildly symptomatic heart failure patients and in asymptomatic patients with left ventricular dysfunction and previous heart failure symptoms. *J Am Coll Cardiol* 2008;**52**:834–43.
3. Moss AJ, Hall WJ, Cannom DS, Klein H, Brown MW, Daubert JP *et al.* Cardiac-resynchronization therapy for the prevention of heart-failure events. *N Engl J Med* 2009;**361**:1329–38.
4. Yu CM, Chan JY, Zhang Q, Omar R, Yip GW, Hussin A *et al.* Biventricular pacing in patients with bradycardia and normal ejection fraction. *N Engl J Med* 2009;**361**:2123–34.
5. Chung ES, Leon AR, Tavazzi L, Sun JP, Nihoyannopoulos P, Merlino J *et al.* Results of the predictors of response to CRT (PROSPECT) trial. *Circulation* 2008;**117**:2608–16.
6. Bleeker GB, Kaandorp TA, Lamb HJ, Boersma E, Steendijk P, de Roos A *et al.* Effect of posterolateral scar tissue on clinical and echocardiographic improvement after cardiac resynchronization therapy. *Circulation* 2006;**113**:969–76.
7. White JA, Yee R, Yuan X, Krahn A, Skanes A, Parker M *et al.* Delayed enhancement magnetic resonance imaging predicts response to cardiac resynchronization therapy in patients with intraventricular dyssynchrony. *J Am Coll Cardiol* 2006;**48**:1953–60.
8. Van de Veire NR, Marsan NA, Schuijf JD, Bleeker GB, Wijffels MC, van Erven L *et al.* Multi-slice computed tomography and noninvasive assessment of left ventricular dyssynchrony by 3-dimensional tissue synchronization imaging in patients with heart failure scheduled for cardiac resynchronization therapy. *Am J Cardiol* 2008;**101**:1023–9.
9. Vogt J, Heinzte J, Lamp B, Hansky B, Horstkotte D. Standard haemodynamic measurements. *Eur Heart J* 2004;**6**(Suppl D):D29–34.
10. Meisel E, Pfeiffer D, Engelmann L, Tebbenjohanns J, Schubert B, Hahn S *et al.* Investigation of coronary venous anatomy by retrograde venography in patients with malignant ventricular tachycardia. *Circulation* 2001;**104**:442–7.
11. Jongbloed MR, Lamb HJ, Bax JJ, Schuijf JD, de Roos A, van der Wall EE *et al.* Noninvasive visualization of the cardiac venous system using multislice computed tomography. *J Am Coll Cardiol* 2005;**45**:749–53.
12. Lumia D, Laganà D, Canì A, Mangini M, Giorgianni A, Cafaro T *et al.* MDCT evaluation of the cardiac venous system. Valutazione mediante TCMS del sistema venoso coronario. *Radiol Med* 2009;**114**:837–51.
13. Nezafat R, Han Y, Peters DC, Herzka DA, Wylie JV, Goddu B *et al.* Coronary magnetic resonance vein imaging: imaging contrast, sequence, and timing. *Magn Reson Med* 2007;**58**:1196–1206.
14. Younger JF, Plein S, Crean A, Ball SG, Greenwood JP. Visualization of coronary venous anatomy by cardiovascular magnetic resonance. *J Cardiovasc Mgn Reson* 2009;**11**:26.
15. Mansour M, Reddy VY, Singh J, Mela T, Rasche V, Ruskin J. Three-dimensional reconstruction of the coronary sinus using rotational angiography. *J Cardiovasc Electrophysiol* 2005;**16**:675–6.
16. Blendea D, Shah RV, Auricchio A, Nandigam V, Orencole M, Heist EK *et al.* Variability of coronary venous anatomy in patients undergoing cardiac resynchronization therapy: a high-speed rotational venography study. *Heart Rhythm* 2007;**4**:1155–62.
17. Blendea D, Mansour M, Shah RV, Chung J, Nandigam V, Heist EK *et al.* Usefulness of high-speed rotational coronary venous angiography during cardiac resynchronization therapy. *Am J Cardiol* 2007;**100**:1561–5.
18. Nölker G, Gutleben KJ, Marschang H, Ritscher G, Asbach S, Marrouche N *et al.* Three-dimensional left atrial and esophagus reconstruction using cardiac C-arm computed tomography with image integration into fluoroscopic views for ablation of atrial fibrillation: accuracy of a novel modality in comparison with multislice computed tomography. *Heart Rhythm* 2008;**5**:1651–7.
19. Rohkohl C, Lauritsch G, Biller L, Prümmer M, Boese J, Hornegger J. Interventional 4D motion estimation and reconstruction of cardiac vasculature without motion periodicity assumption. *Medical Image Analysis* 2010;**14**:687–94.
20. Kofune M, Watanabe I, Ashino S, Okumura Y, Kawauchi K, Kofune T *et al.* Three-dimensional reconstruction of the coronary sinus with rotational angiography. *Circ J* 2008;**72**:1020–1.
21. Gutleben KJ, Marschang H, Sinha AM, Schmidt M, Ritscher G, Rittger H *et al.* Selective cannulation of posterolateral veins in cardiac resynchronization therapy: a new access that shortens procedure times. *Heart Rhythm* 2008;**5**(Suppl):S339 (Abstr).
22. Duray GZ, Hohnloser SH, Israel CW. Coronary sinus side branches for cardiac resynchronization therapy: prospective evaluation of availability, implant success, and procedural determinants. *J Cardiovasc Electrophysiol* 2008;**19**:489–95.